Progress In Electromagnetics Research, PIER 79, 401–413, 2008

PERFORMANCE OF IMPULSE RADIO UWB COMMUNICATIONS BASED ON TIME REVERSAL TECHNIQUE

X. Liu, B.-Z. Wang, S. Xiao, and J. Deng

Institute of Applied Physics
University of Electronic Science and Technology of China
Chengdu 610054, China

Abstract—In this paper, the bit-error-rates performance of impulse radio ultra-wideband (IR-UWB) wireless communication system based on time reversal technique is investigated in both single-input single-output and multiple-input single-output situations. Simulations indicate that the good result is obtained as we expect it and IR-UWB based on time reversal technique is very promising for high bit rates wireless communication applications.

1. INTRODUCTION

In recent ultra-wideband (UWB) [1–3, 16–18] communication topics, time reversal (TR) technique [4, 5, 19] is expected to become a promising solution in minimizing multi-path and channel fading thus improving the signal-to-noise ratio (SNR) and reducing the inter-symbol interference (ISI). [6–9] show the applications of TR-UWB. [10] proposed an MMSE-TR equalizer in UWB communications and investigated the benefit of temporal focusing. The authors in [11, 12] evaluated the applicability of multi-user TR-UWB communication in improving the multi-user system capacity and communication range. Combined with TR technique, the Impulse Radio-UWB (IR-UWB) systems have no need to use the Rake receiver to obtain good demodulation performance. Therefore, it reduces the complexity of the system structure, especially the receiver devices. In addition, this technique might potentially increase the effective Shannon channel capacity when we deal with multi-user UWB communications. These advantages are brought in by the two important characteristics: the temporal focusing and the spatial focusing.

In this paper, we discuss the improvement of IR-UWB wireless communications by introducing TR technique. We try to use TR in most of the existing IR-UWB schemes. Different modulation schemes, pulse position modulation (PPM) and pulse amplitude modulation (PAM), are investigated. Two common multiple access schemes, Time-Hopping (TH) and Direct Sequence (DS), are considered. IEEE 802. 13. 3a [14, 15] channel model is used to simulate the multi-path UWB channel environment. Quantificationally, we focus on evaluating the performance of IR-UWB wireless communication systems based on TR technique. The results present the advantages of the new systems.

The paper is organized as follows. Section 2 details the fundamental theory of Time-Reversal technique. The concept behind the TR-IR-UWB communications is discussed. In Section 3, system performances are presented in term of bit-error-rates (BER). Section 4 is the conclusion.

2. BASIC CONCEPT OF THE TR-IR-UWB

Time-reversal, or phase conjugation in the frequency domain, can be seen as a pre-equalizer. It implements a matched filter of the impulse response of the UWB channel. We assume the transmitted signal as $x(t)$ and denote the channel impulse response (CIR) by $h_{r_0}(t)$ at the intended receiver, where r_0 is the receiver location and t is the delay variable. Then the received signal at discretional position r can be written as:

$$r(t) = x(t) \otimes h_r(t) \otimes h_{r_0}(-t) + n(t) \tag{1}$$

where $h_{r_0}(-t)$is the time reversal of CIR, $\otimes$ denotes convolution with respect to the delay variable. $R_{r,r_0}(t) = h_r(t) \otimes h_{r_0}(-t)$ can be seen as the pre-filter CIR. $n(t)$ is usually additive white Gaussian noise with a double -sideband power spectral density of $N_0/2$.

According to [13], different modulation schemes (PPM, PAM) and spreading spectrum schemes (DS, TH) result in different general expressions. They are summarized as follows

$$\mathrm{TH-PPM}: x(t) = \sum_{j=-\infty}^{+\infty} p(t - jT_s - \eta_j - a_j\varepsilon) \tag{2}$$

$$\mathrm{TH-PAM}: x(t) = \sum_{j=-\infty}^{+\infty} p_{a_j}(t - jT_s - \eta_j) \tag{3}$$

$$\mathrm{DS-PAM}: x(t) = \sum_{j=-\infty}^{+\infty} d_j p(t - jT_s) \tag{4}$$

$$\mathrm{DS-PPM}: x(t) = \sum_{j=-\infty}^{+\infty} p\left(t - jT_s - \varepsilon\frac{d_j+1}{2}\right) \tag{5}$$

where $a_j \in \{0,1\}$, $d_j \in \{-1,+1\}$, $p(t)$ is the impulse response of the pulse generator, it could be a Gaussian pulse or its high order derivative. T_s is the pulse period, ε is PPM shift and η_j is the time shift of the jth pulse determined by time-hoping codes.

As widely used, the CIR of IEEE proposed UWB multi-path channel model can be written as

$$h_{r_0}(t) = X_{r_0}\sum_{n=1}^{N}\sum_{k=1}^{K_{(n)}}\alpha_{nk}^{r_0}\delta\left(t - T_n^{r_0} - \tau_{nk}^{r_0}\right) \tag{6}$$

where X_{r_0} represents the log normal fading, N is the number of clusters and $K_{(n)}$ is the number of multi-paths in the nth cluster. $\alpha_{nk}^{r_0}$ are the multi-path gain coefficients, $T_n^{r_0}$ is the delay of the nth cluster, $\tau_{nk}^{r_0}$ is the delay of the kth multi-path component relative to the nth cluster arrival time $T_n^{r_0}$.

Then the pre-filter CIR R_{r,r_0} is given by

$$\begin{aligned} R_{r,r_0}(t) &= h_r(t)\otimes h_{r_0}(-t) \\ &= \left[X_r\sum_{n=1}^{N_r}\sum_{k=1}^{K_{r(n)}}\alpha_{nk}^{r}\delta(t - T_n^{r} - \tau_{nk}^{r})\right] \\ &\quad\otimes\left[X_{r_0}\sum_{\eta=1}^{N_{r_0}}\sum_{\xi=1}^{K_{r_0(\eta)}}\alpha_{\eta\xi}^{r_0}\delta(-t - T_\eta^{r_0} - \tau_{\eta\xi}^{r_0})\right] \\ &= X_rX_{r_0}\sum_{n=1}^{N_r}\sum_{k=1}^{K_{r(n)}}\alpha_{nk}^{r}\sum_{\eta=1}^{N_{r_0}}\sum_{\xi=1}^{K_{r_0(\eta)}}\alpha_{\eta\xi}^{r_0}\delta(t - T_n^{r} - \tau_{nk}^{r} + T_\eta^{r_0} + \tau_{\eta\xi}^{r_0}) \end{aligned} \tag{7}$$

The above formulation denotes the pre-equalized CIR of the TR-IR-UWB system when the receiver antenna is placed at any location. But we concern mainly the point-to-point communication problems, which include single-input single-output (SISO) and multiple-input single-output (MISO) systems in our discussion. Under this precondition, the receiver antenna's location $r = r_0$ and (7) can be rewritten as

$$\begin{aligned} R_{r_0,r_0}(t) &= h_{r_0}(t)\otimes h_{r_0}(-t) \\ &= X_{r_0}^2\sum_{n=1}^{N_{r_0}}\sum_{k=1}^{K_{r_0(n)}}\alpha_{nk}^{r_0}\sum_{\eta=1}^{N_{r_0}}\sum_{\xi=1}^{K_{r_0(\eta)}}\alpha_{\eta\xi}^{r_0}\delta(t - T_n^{r_0} - \tau_{nk}^{r_0} + T_\eta^{r_0} + \tau_{\eta\xi}^{r_0}) \end{aligned} \tag{8}$$

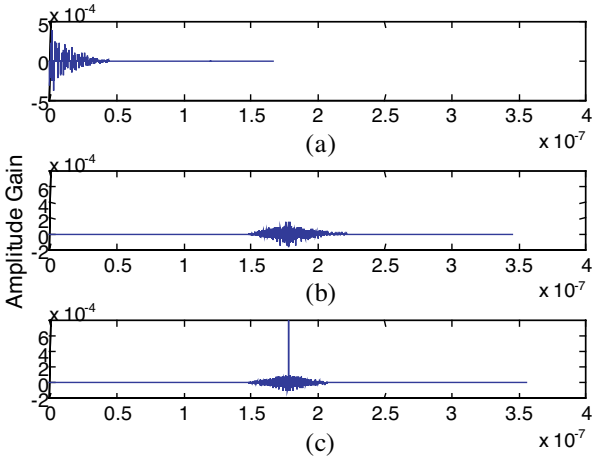

Figure 1. (a) Traditional UWB multi-path channel impulse response h_{r_0}, (b) the nearby position time reversed channel impulse response $R_{r,r_0}(r \neq r_0, |r| = |r_0|)$, (c) the intended position time reversed channel impulse response R_{r_0,r_0}.

Equation (8) indicates that the time-reversed CIRs' main peak is at $t = (T_n^{r_0} + \tau_{nk}^{r_0})\big|_{\max} 1 \leq n \leq N_{r_0},\ 1 \leq k \leq K_{r_0(n)}$ and it captures most of the total energy of the transmitted signal. Then this clearly characterizes the temporal focusing of the TR technique. On the other hand, if another receiver antenna is located beyond the intended receiver antenna ($r \neq r_0$), the main peak of $R_{r,r_0}(t)$ is smaller than $R_{r_0,r_0}(t)$ in large amount. So the nearby antenna receives a small quantity of signal energy, and it is how the spatial focusing works. Fig. 1 shows the traditional UWB CIR, the nearby position TR CIR and the intended position TR CIR. r of the nearby position is set to be having the same distance with r_0 and the relative position can not be get exactly because IEEE channel model is a statistical model. If we want to study more about spatial focusing performance attenuation caused by offset distance, we should change the method of CIR generation and bring some relative factors between r and r_0 according to real channel environment.

By inserting (8) into (1), the received signal of SISO system can be obtained

$$r(t) = X_{r_0}^2 \sum_{n=1}^{N_{r_0}} \sum_{k=1}^{K_{r_0(n)}} \alpha_{nk}^{r_0} \sum_{\eta=1}^{N_{r_0}} \sum_{\xi=1}^{K_{r_0(\eta)}} \alpha_{\eta\xi}^{r_0} x(t - T_n^{r_0} - \tau_{nk}^{r_0} + T_\eta^{r_0} + \tau_{\eta\xi}^{r_0}) + n(t) \tag{9}$$

while the received signal of MISO system can be

$$\begin{aligned} r(t) \;=\; & X_{r_0}^2 \sum_{n=1}^{N_{r_0}} \sum_{k=1}^{K_{r_0(n)}} \alpha_{nk}^{r_0} \sum_{\eta=1}^{N_{r_0}} \sum_{\xi=1}^{K_{r_0(\eta)}} \alpha_{\eta\xi}^{r_0} x(t - T_n^{r_0} - \tau_{nk}^{r_0} + T_\eta^{r_0} + \tau_{\eta\xi}^{r_0}) \\ & + \sum_{j=1}^{N_{users}-1} \left\{ X_{r_j} X_{r_0} \sum_{n=1}^{N_{r_j}} \sum_{k=1}^{K_{r_j(n)}} \alpha_{nk}^{r_j} \right. \\ & \left. \sum_{\eta=1}^{N_{r_0}} \sum_{\xi=1}^{K_{r_0(\eta)}} \alpha_{\eta\xi}^{r_0} \delta(t - T_n^{r_j} - \tau_{nk}^{r_j} + T_\eta^{r_0} + \tau_{\eta\xi}^{r_0}) \right\} + n(t) \end{aligned} \tag{10}$$

It includes 3 parts. The first part is useful signal. The second part is multi-input interference. And the third part is noise signal.

3. PERFORMANCE OF TR-IR-UWB

This section will discuss the performance of TR based SISO IR-UWB and MISO IR-UWB systems in typical line of sight (LOS) and non line of sight (NLOS) channels respectively. The typical IEEE UWB channel model parameters and characteristics are listed in Table 1 [14], which was found using measurement data based on couple of channel characteristics for different channel models. where $NP_{10\,\mathrm{dB}}$ is the number of paths within 10 dB of the strongest path and $NP_{(85\%)}$ gives the number of paths containing 85 percent of the energy. σ_1 (dB) is standard deviation of cluster log-normal fading term, σ_2 (dB) is standard deviation of ray log-normal fading term, σ_x (dB) is standard deviation of log-normal shadowing term for total multi-path realization.

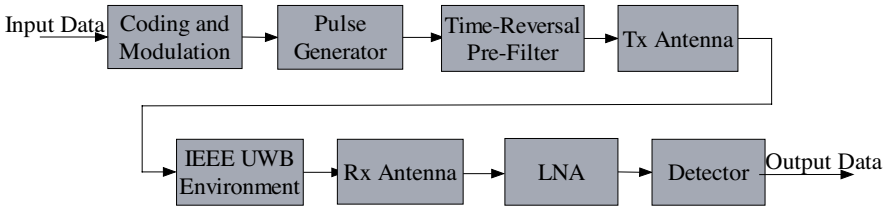

Figure 2. Simplified block diagram for SISO TR-IR-UWB system.

Table 1. Channel characteristics and parameters.

Target Channel Characteristics	CM1	CM2	CM3	CM4
Distance (m)	0-4	0-4	4-10	
(Non-)line of sight	LOS	NLOS	NLOS	NLOS
Mean excess delay (ns) (τ_m)	5.05	10.38	14.18	
RMS delay (ns) (τ_{rms})	5.28	8.03	14.28	25
$NP_{10\,\mathrm{dB}}$			35	
$NP_{(85\%)}$	24	36.1	61.54	
Model Parameters				
Cluster arrival rate (Λ)	0.0233	0.4	0.0667	0.0667
Ray arrival rate (λ)	2.5	0.5	2.1	2.1
Cluster decay factor (Γ)	7.1	5.5	14.00	24.00
Ray decay factor (γ)	4.3	6.7	7.9	12
σ_1 (dB)	3.3941	3.3941	3.3941	3.3941
σ_2 (dB)	3.3941	3.3941	3.3941	3.3941
σ_x (dB)	3	3	3	3

3.1. SISO TR-IR-UWB Systems

A simplified block diagram of the system structure is shown in Fig. 2. In practical design, the pulse generating and time reversal process are realized at the same time. However, in our simulation setup, the time reversal process is carried out after pulse generating. We just promise that the time reversal of CIR implements the TR pre-filter according to Section 2. It's an equivalent model. A low-noise-amplifier (LNA) with a gain of 0 dB is used here.

We simulate the communication system and investigate the bit-error-rates (BER) versus the signal-to-noise ratio (Ex/No). The results obtained here are compared with the results given by UWB system with Rake receiver. The most common Rake receivers are the selective Rake (SRake) and the partial Rake (PRake). The SRake selects the L largest paths out of the available resolved multipath components and then combines them using maximal-ratio combining (MRC). Compared with the SRake, the PRake is easier to be realized because it just selects the L first arriving paths components and then combines them using MPC. Obviously, the SRake has better performance than the PRake. So the SRake structure is adopted in this paper and the SRake structure is shown in Fig. 3. L is the number of the correlators, which are called Rake fingers. $m_i(t)$ is the ith finger's correlation mask. ω_i denotes the weighted parameter according to the receiver scheme.

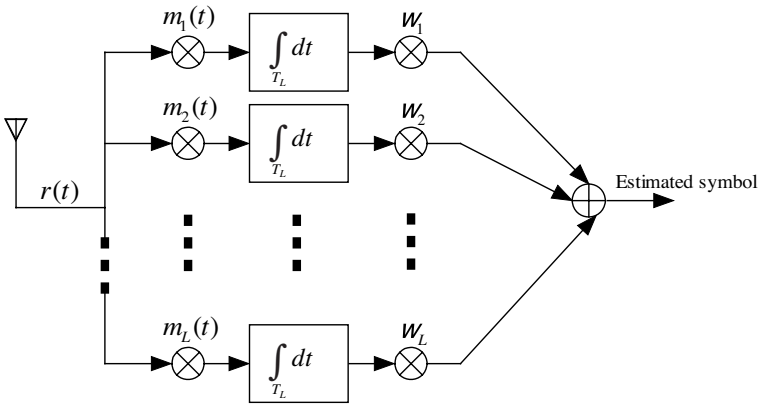

Figure 3. The SRake structure with L Rake fingers.

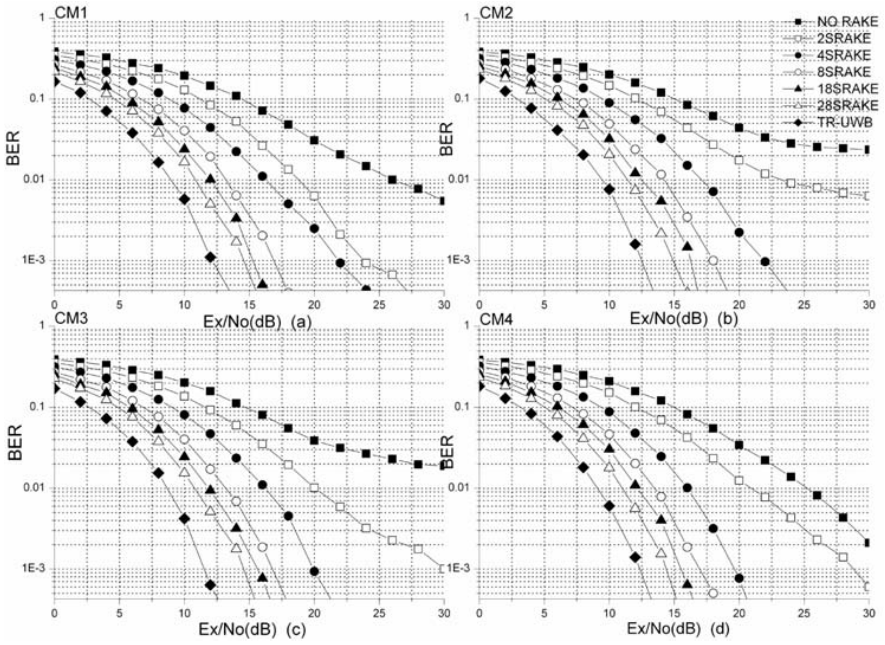

Figure 4. BER performances (using TH-PPM scheme) of SISO TR-IR-UWB system and usual SISO UWB system with L selective Rake fingers receiver (LSRAKE) (a) in CM1 channel (b) in CM2 channel (c) in CM3 channel (d) in CM4 channel.

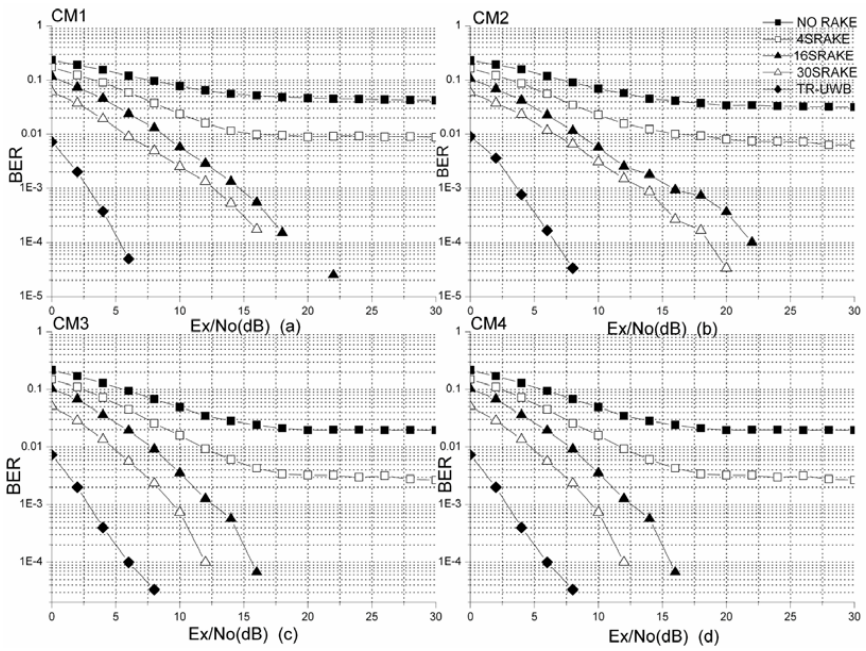

Figure 5. BER performances (using DS-PAM scheme) of SISO TR-IR-UWB system and usual SISO UWB system with L selective Rake fingers receiver (LSRAKE) (a) in CM1 channel (b) in CM2 channel (c) in CM3 channel (d) in CM4 channel.

A repetition code for the input data stream is generated by the repetition coder to efficiently improve the BER performances of both traditional UWB system and TR UWB system. TH-PPM scheme and DS-PAM scheme are employed and evaluated. Fig. 4 and Fig. 5 present the BER performances of them respectively. The basic simulation parameters are listed here: sampling frequency $f_s = 50 \times 10^9$ Hz, average transmitted power $A_{pow} = -30$ dB, average pulse repetition period $t_s = 60 \times 10^{-9}$ s, number of pulses per bit $N_s = 9$, PPM time shift $dPPM = 0.5 \times 10^{-9}$ s, chip time for TH-PPM $t_c = 1 \times 10^{-9}$ s, periodicity of TH code for TH-PPM $N_{pth} = 5$, cardinality of the TH code $N_c = 5$, periodicity of DS code $N_{pds} = 10$. It could be seen that the TR based SISO system, as we expected, has much better BER performance than usual UWB system in all four channels and in both TH-PPM and DS-PAM cases. Fig. 6 answers the question: how many Rake fingers should be used if usual systems want to get as good performance as TR based system? For TH-PPM scheme, the usual

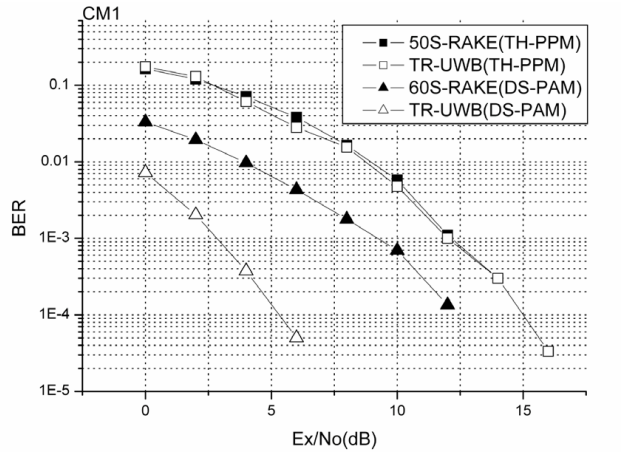

Figure 6. Using more RAKE fingers in usual UWB system to obtain equivalent performance to TR-IR-UWB system.

system can obtain equivalent performance by using about 50 fingers. However, it's difficult for DS-PAM scheme even though 60 more fingers are used.

3.2. MISO TR-IR-UWB Systems

Figure 7 shows the block diagram for MISO TR-IR-UWB system. The J input data streams are denoted as $Input\,data1$-$Input\,dataJ$. IEEE UWB channel model is still used here. The detector is controlled by the receiver template controller to demodulate different transmittal user data by turns.

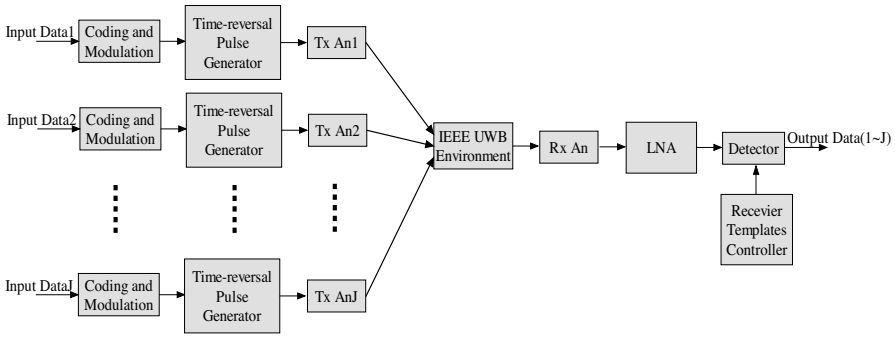

Figure 7. Simplified block diagram for MISO TR-IR-UWB system.

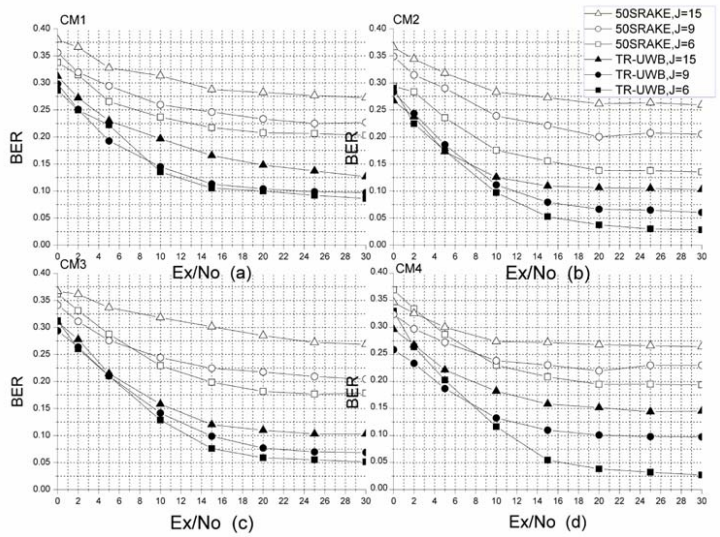

Figure 8. BER performances (using TH-PPM scheme) of MISO TR-IR-UWB system and usual MISO UWB system with 50 selective Rake fingers receiver (a) in CM1 channel (b) in CM2 channel (c) in CM3 channel (d) in CM4 channel.

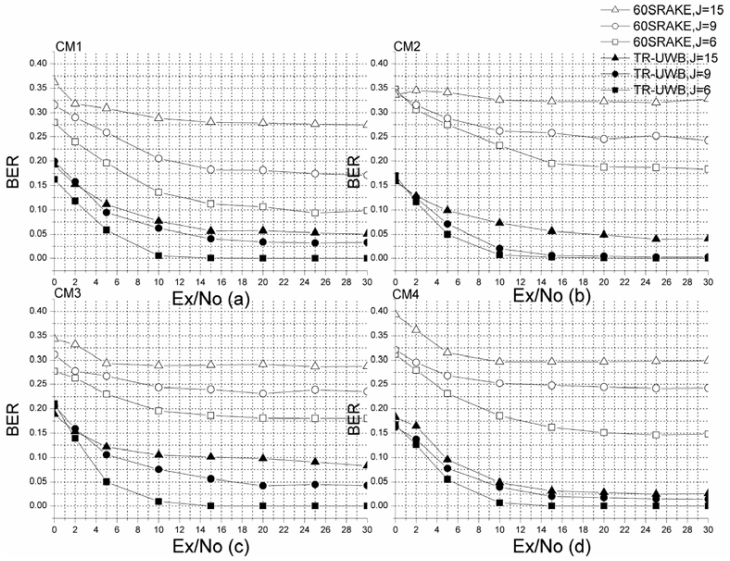

Figure 9. BER performances (using DS-PAM scheme) of MISO TR-IR-UWB system and usual MISO UWB system with 60 selective Rake fingers receiver (a) in CM1 channel (b) in CM2 channel (c) in CM3 channel (d) in CM4 channel.

In the above subsection, we discussed how to get as good performance as TR-IR-UWB system in usual TH-PPM and DS-PAM SISO UWB system by increasing the number of Rake fingers. According to the results shown in Fig. 6, we use 50 fingers in traditional TH-PPM MISO system and 60 fingers in DS-PAM MISO system for comparison with the MISO TR-IR-UWB system. 6, 9, and 15 users are investigated here, i.e., $J = 6, 9, 15$. Each transmitter has the same simulation setup as the SISO situation. The BER performances are presented in Figs. 8 and 9. The results hold the promise of the TR based UWB systems.

4. CONCLUSIONS

The performances of time-reversal technique based UWB wireless systems are investigated for future communication application in this paper. The temporal focusing and the spatial focusing of time reversal make the energy collection increase and improve the performance of UWB system. TR is proved to be effective and promising in high bit rates wireless communication applications, especially in impulse radio UWB applications.

There are many other issues should be studied in this filed. They are power spectral density of the transmitted signal, synchronization of the system and so on. We will discuss some of them in our next report.

ACKNOWLEDGMENT

This work was supported by the Hi-Tech Research and Development Program of China (2006AA01Z275), the national nature science foundation of China (60501011, 90505001), and the Creative Research Team Program of UESTC.

REFERENCES

1. Win, M. Z. and R. A. Scholtz, "Impulse radio: How it works," *IEEE Commun. Lett.*, Vol. 2, No. 2, 36–38, Feb. 1998.
2. Chen, F. C. and W. C. Chew, "Time-domain ultra-wideband microwave imaging radar system," *Journal of Electromagnetic Waves and Applications*, Vol. 17, 313–331, 2003.
3. Fan, Z., L. X. Ran, and J. A. Kong, "Source pulse optimizations for UWB radio systems," *Journal of Electromagnetic Waves and Applications*, Vol. 20, 1535–1550, 2006.

4. Fink, M., "Time reversal of ultrasonic fields. I. Basic principles," *IEEE Trans. Ultrason. Ferroelectr. Freq. Control.*, Vol. 39, No. 5, 555–566, Sept. 1992.
5. Chen, X., "Time-reversal Operator for a small sphere in electromagnetic fields," *Journal of Electromagnetic Waves and Applications*, Vol. 21, 1219–1230, 2007.
6. Win, M. Z. and R. A. Scholtz, "On the robustness of ultra-wide bandwidth signals in dense multipath environments," *IEEE Commun. Lett.*, Vol. 2, 51–53, Feb. 1998.
7. Qiu, R. C., "A Generalized time domain multipath channel and its applications in ultra-wideband (UWB) receiver design: System performance analysis," *Proc. IEEE Wireless Comm. Network Conf., 2004*, Vol. 3, No. 6, 2312–2324, Mar. 2004.
8. Kyristi, P., G. Panicolaou, and A. Oprea, "MISO time reversal and delayspread compression for FWA channels at 5 GHz," *IEEE Antennas Wireless Propag. Lett.*, Vol. 3, 96–99, Dec. 2004.
9. Xiao, S., J. Chen, B.-Z. Wang, and X.-F. Liu, "A Numerical study on time- reversal electromagnetic wave for indoor ultra-wideband signal transmission," *Progress In Electromagnetics Research*, PIER 77, 329–342, 2007.
10. Strohmer, T., M. Emami, J. Hansen, G Papanicolaou, and A. J. Paulraj, "Application of time-reversal with MMSE equalizer to UWB communictions," *Proc. IEEE Global Telecommunications Conference, 2004. GLOBECOM'04*, Vol. 5, 3123–3127, Dec. 2004.
11. Nguyen, H. T., I. Z. Kovcs, and P. C. F. Eggers, "A time reversal transmission approach for multiuser UWB communications," *IEEE Trans. Antennas Propagat.*, Vol. 54, No. 11, 3216–3224, Nov. 2006.
12. Qiu, R. C., C. M. Zhou, N. Guo, and J. Q. Zhang, "Time reversal with MISO for ultrawideband communications: Experimental results," *IEEE Antennas Wireless Propag. Lett.*, Vol. 5, 269–275, Dec. 2006.
13. Benedetto, M. G. D. and G. Giancola, *Understanding Ultra Wide Band Radio Fundamentals*, Prentice Hall, Upper Saddle River, NJ, 2004.
14. Foester, J., "Channel modeling sub-committee report final (doc: IEEE 802-15-02/490r1-SG3a)," *IEEE P802.15 Working Group for Wireless Personal Area Networks (WPANs)*, Feb. 2002.
15. Cramer, R. J.-M., R. A. Scholtz, and M. Z. Win, "Evaluation of an indoor ultra-wideband propagation channel (doc: IEEE 802-15-02/286r0-SG3a)," *IEEE P802.15 Working Group for Wireless*

Personal Area Networks (WPANs), June 2002.

16. Zhou, L.-L., H.-B. Zhu, and N.-T. Zhang, "Iterative solution to the noyched waveform design in cognitive ultra-wideband radio system," *Progress In Electromagnetic Research*, PIER 75, 271–284, 2007.
17. Chen, C.-H., C.-H. Liu, C.-C. Chiu, and T.-M. Hu, "Ultra-wide band channel caculation by SBR/IMAG techniques for indoor communication," *Journal of Electromagnetic Waves and Applications*, Vol. 20, No. 1, 41–51, 2006.
18. Soliman, M. S., T. Morimoto, and Z.-I. Kawasaki, "Three-dimensioal localization system for impulsice noise sources using ultra-wdieband digital interferometer techniquie," *Journal of Electromagnetic Waves and Applications*, Vol. 20, No. 4, 515–530, 2006.
19. Candy, J. V., D. H. Chambers, C. L. Robbins, et al., "Wideband multichannel time-reversal processing for acoustic communications in highly reverberant environments," *Journal of the Acoustical Society of America*, Vol. 120, 838–851, 2006.